Biophysical Journal Volume 73 November 1997 2304–2312

Temperature-Induced Structural Changes in the Myosin Thick Filament of Skinned Rabbit Psoas Muscle

S. Malinchik, S. Xu, and L. C. Yu

Laboratory of Physical Biology, National Institute of Arthritis and Musculoskeletal and Skin Diseases, National Institutes of Health, Bethesda, Maryland 20892 USA

ABSTRACT By using synchrotron radiation and an imaging plate for recording diffraction patterns, we have obtained high-resolution x-ray patterns from relaxed rabbit psoas muscle at temperatures ranging from 1°C to 30°C. This allowed us to obtain intensity profiles of the first six myosin layer lines and apply a model-building approach for structural analysis. At temperatures 20°C and higher, the layer lines are sharp with clearly defined maxima. Modeling based on the data obtained at 20°C reveals that the average center of the cross-bridges is at 135 Å from the center of the thick filament and both of the myosin heads appear to wrap around the backbone. At 10°C and lower, the layer lines become very weak and diffuse scattering increases considerably. At 4°C, the peak of the first layer line shifts toward the meridian from 0.0047 to 0.0038 $Å^{-1}$ and decreases in intensity approximately by a factor of four compared to that at 20°C, although the intensities of higher-order layer lines remain ~10–15% of the first layer line. Our modeling suggests that as the temperature is lowered from 20°C to 4°C the center of cross-bridges extends radially away from the center of the filament (135 Å to 175 Å). Furthermore, the fraction of helically ordered cross-bridges decreases at least by a factor of two, while the isotropic disorder (the temperature factor) remains approximately unchanged. Our results on the order/disordering effects of temperature are in general agreement with earlier results of Wray [Wray, J. 1987. Structure of relaxed myosin filaments in relation to nucleotide state in vertebrate skeletal muscle. *J. Muscle Res. Cell Motil.* 8:62*a* (Abstr.)] and Lowy et al. (Lowy, J., D. Popp, and A. A. Stewart. 1991. X-ray studies of order–disorder transitions in the myosin heads of skinned rabbit psoas muscles. *Biophys. J.* 60:812–824). and support Poulsen and Lowy's hypothesis of coexistence of ordered and disordered cross-bridge populations in muscle (Poulsen, F. R., and J. Lowy. 1983. Small angle scattering from myosin heads in relaxed and rigor frog skeletal muscle. *Nature (Lond.).* 303:146–152.). However, our results added new insights into the disordered population. Present modeling together with data analysis (Xu, S., S. Malinchik, Th. Kraft, B. Brenner, and L. C. Yu. 1997. X-ray diffraction studies of cross-bridges weakly bound to actin in relaxed skinned fibers of rabbit psoas muscle. *Biophys. J.* 73:000–000) indicate that in a relaxed muscle, cross-bridges are distributed in three populations: those that are ordered on the thick filament helix and those that are disordered; and *within the disordered population*, some cross-bridges are detached and some are weakly attached to actin. One critical conclusion of the present study is that the apparent order ↔ disorder transition as a function of temperature is not due to an increase/decrease in thermal motion (temperature factor) for the entire population, but a redistribution of cross-bridges among the three populations. Changing the temperature leads to a change in the fraction of cross-bridges located on the helix, while changing the ionic strength at a given temperature affects the disordered population leading to a change in the relative fraction of cross-bridges detached from and weakly attached to actin. Since the redistribution is reversible, we suggest that there is an equilibrium among the three populations of cross-bridges.

INTRODUCTION

The contractile system of vertebrate striated muscle consists of interdigitating arrays of myosin containing thick filaments and actin containing thin filaments. It is generally accepted that force is generated by projections from the myosin filaments (cross-bridges) attaching to and pulling on the actin filaments. The structure of the thin filaments is reasonably well understood at the molecular level (Kabsch et al., 1990; Holmes et al. 1990), but much less detail is known about the structure of the thick filaments.

It is well known that myosin cross-bridges occur at an average interval of 143 Å in a three-stranded helical arrangement with an axial repeat of 430 Å (Huxley and Brown, 1967; Squire, 1981; Ip and Heuser, 1983; Stewart and Kensler, 1986; Knight and Trinick, 1984). In some skeletal muscles the thick filaments are well-ordered along the fiber axis, and it is possible to obtain well-resolved x-ray diffraction patterns containing information about the shape and the orientation of individual cross-bridges. Thus far, interpretations and modeling of the thick filaments in vertebrate muscles have been mostly based on diffraction patterns obtained from, e.g., the intact relaxed frog muscles (Haselgrove, 1980; Malinchik and Lednev, 1992), and bony fish muscle (Harford and Squire, 1986). Knowledge of the thick filaments in the rabbit (mammalian) skeletal muscle, however, remains limited.

Some features of the thick filaments in the skinned relaxed rabbit muscle have been reported. The x-ray diffraction patterns were found to be very sensitive to temperature:

Received for publication 10 February 1997 and in final form 4 August 1997.

Address reprint requests to L. Yu at the Laboratory of Physical Biology, National Institute of Arthritis and Musculoskeletal and Skin Diseases, National Institutes of Health, Bethesda, MD 20892. Tel.: 301-496-5415; Fax: 301-402-0009; E-mail: lcyu@helix.nih.gov.

Dr. Malinchik's present address is Department of Biology, Boston College, Chestnut Hill, MA 02167. E-mail: sergey@abby.bc.edu.

0006-3495/97/11/2304/09 $2.00

at room temperature the relaxed muscle gives clear myosin layer lines (Wray, 1987; Wakabayashi et al., 1988; Lowy et al., 1991), which decrease considerably in intensity with lowering of the temperature. The loss of the helical order appears to be reversible (Wray, 1987). It was demonstrated (Lowy et al., 1991) that the relationship between the intensities of the layer lines and the diffuse scattering is of an inverse nature, and that the transition occurs over a narrow temperature range (12–14°) with a sigmoidal function. Poulsen and Lowy (1983) explained the phenomenon of simultaneous existence of myosin layer lines and diffuse scattering in terms of two populations of myosin heads. One population consists of helically ordered cross-bridges that produce myosin layer lines on x-ray diffraction patterns. Another population consists of disordered cross-bridges mainly accounting for the diffuse scattering. Our recent results (Xu et al., 1997) added new insight into the disordered population. At all temperatures studied thus far (1–30°C) in a skinned relaxed rabbit psoas muscle, some cross-bridges within the disordered population are weakly attached to actin, while some are detached. The attached cross-bridges assume orientations that are hardly distinguishable from the detached and disordered cross-bridges.

Due to a lack of experimental data with adequate signals for quantitative analysis, structure of the ordered cross-bridge population has not been studied, quantitative estimation of the ratio between ordered/disordered populations at different temperatures has not been reported, and the nature of changes in the thick filament as a function of temperature is not understood.

We have obtained high-resolution x-ray diffraction patterns from skinned rabbit psoas muscle in a wide range of temperatures (from 1° to 30°C) (see also Xu et al., 1997). Intensity profiles of myosin layer lines at 20°C and 4°C were analyzed in detail. A model of the helical arrangement of the cross-bridges at 20°C as well as some changes as a function of temperature are presented. A quantitative estimate of the relative distribution of the ordered and the disordered populations is provided at the two temperatures. Preliminary results were reported previously (Malinchik et al., 1996; Xu et al., 1996)

METHODS

X-ray diffraction experiments

Chemically skinned single bundles of the rabbit M. psoas muscle fibers were used in all x-ray experiments. Sarcomere length was 2.5 μm and the ionic strength (μ) was either 150 mM or 170 mM. Details of our specimen preparation and protocol of the x-ray diffraction experiments are described in the accompanying paper (Xu et al., 1997). The x-ray patterns presented in this paper were obtained on synchrotron beamline X13 of the European Molecular Biology Laboratory at DESY, Hamburg, Germany. Fuji imaging plates (Fuji, Japan) with 100 × 100 μm pixel size were used to record patterns. The crystal-mirror focusing camera had the specimen-to-plate distance of 2840 mm. Each pattern generally had exposure time of 4 min and the total exposure time for each bundle did not exceed 20 min. The main features of our experiments are the following: 1) the sarcomere length was determined by laser diffraction; 2) during exposure the solution containing the ATP regenerating system was continuously pumped to keep it homogeneous and the temperature uniform along the muscle bundle; 3) tension was monitored during exposure to ensure that it was <2% of the estimated maximal active force; 4) the specimen was moved along the fiber axis during the exposure to reduce x-ray damage. For direct comparison of absolute intensity changes, the successive diffraction patterns were taken from single bundles, each with temperature changed in random order. The patterns recorded under the same conditions were added to increase the signal-to-noise ratio (for more details, see Xu et al., 1997).

Data reduction and analysis

The data were displayed and analyzed on Silicon Graphics Indigo workstations using a modified version of the Profida program written by Michael Lorenz (MPI, Heidelberg, Germany). The program was adjusted to the size of our patterns (2000 by 2000 pxs). It rotates and translates the x-ray patterns to ensure that the meridian is vertical and the center of the diagram is in the origin of Cartesian coordinates. Two symmetrically located meridional reflections ("215 Å" or "143 Å") and equatorial [1, 0] or [1, 1] reflections were usually used to center the pattern.

Integrated intensity profiles in the vertical and horizontal direction were taken after averaging four or three quadrants of the x-ray pattern. The vertical widths of the slices for the profiles were chosen to include the whole reflection area. To obtain the intensity profiles along the layer lines at room temperature, three horizontal (parallel to the equator) cuts were made: one wide cut centering around the layer line itself, and two other narrow cuts, one below and one above the first cut, used for background estimation. The two narrow cuts were averaged and scaled by the widths of the cuts. The resulting profile was found to be a good approximation for the background profile along the layer line and was subtracted from the layer line profile. After background "smoothing" and subtraction, PeakFit software (Jendel Scientific, Inc. SPSS, Inc., Chicago, IL) was used to fit the stripped data and determine the exact positions of the peaks on the layer lines.

For analysis of the intensities of the weak layer lines (for low temperature patterns), a set of vertical cuts normally 0.001 $Å^{-1}$ in width were made perpendicular to the layer lines. The cuts were contiguous and together they covered a wide region in the radial direction, ranging approximately from 0 to 0.014 $Å^{-1}$.

The profiles of the vertical cuts were displayed and analyzed by the PCA program (Nucleus, Inc., Oak Ridge, TN). Integrated intensities and positions of the centroids of the peaks on the vertical profiles were measured after subtracting the background. The intensity profiles along each layer line in the radial direction were thus reconstructed (see Xu et al., 1997).

Model calculations

The thick filament structure was assumed to consist of a smooth cylindrical backbone and three-stranded helix of myosin cross-bridges with an axial period of 429 Å. The backbone of the myosin filament was assumed not to contribute to the diffraction pattern except to the equatorial reflections (see Discussion). The cross-bridges were described in terms of overlapping spheres. The size and polar coordinates of each sphere were defined to simulate the desired model (see below). For an unsampled array of helical objects, the observed pattern is the same as the rotationally averaged pattern from one filament. The intensity of each layer line (l) at a reciprocal radius (R) is the sum of the intensities of the individual Bessel orders on each layer line (Franklin and Klug, 1955). Thus

$$\langle I_l(R)\rangle_\psi = \sum_n |F_{nl}(R)|^2$$

The Bessel orders (n) on the layer lines (l) are: 1st and 4th: 3, −6, 12; 2nd and 5th: −3, 6, −12; 3rd and 6th: 0, 9, −9.

$$F_{nl}(R) = \sum_j f_j J_n(2\pi r_j R)\exp i\left[n\left(\frac{\pi}{2} - \phi_j\right) + \frac{2\pi l z_j}{c}\right]$$

where r_j, ϕ_j, and z_j are cylindrical coordinates of the jth sphere; f_j is the structural factor of the sphere:

$$f_j(R) = 4\pi r_j^3 \frac{\sin(2\pi r_j R) - (2\pi r_j R)\cos(2\pi r_j R)}{(2\pi r_j R)^3}$$

The model of the cross-bridge used for simulating the layer line is the following. The main parameters determining cross-bridge configuration in the cylindrical system of coordinates are the angles, α_{1or2}, β_{1or2}; and radii, r_{1or2}, for each head, correspondingly (see Fig. 1). The individual cross-bridge is assumed to be a V-shape, i.e., the tail ends of the two heads are considered to be very close to each other to ensure a permanent transition into the coiled-coil structure of the S2 fragment. This configuration implies that r_1 and r_2 are related parameters, and as a varying parameter we used the averaged radius, $r_c = (r_1 + r_2)/2$, to characterize the radial distance of the cross-bridge as a whole from the center of the filament. Another parameter used in the fitting procedure is root mean square (r.m.s.) isotropic displacement, Δ, of the heads from equilibrium positions, which characterizes the first type of disordering effects (Vainshtein, 1966). At the final stage of fitting, the isotropic disordering was replaced by two disordering parameters in radial and axial directions, Δ_r and Δ_z, correspondingly. The intensity calculated for the single thick filament is multiplied by an exponential term

$$\exp(-4\pi^2\Delta^2[R^2 + (l/c)^2])$$

or

$$\exp(-4\pi^2[\Delta_r^2 R^2 + \Delta_z^2(l/c)^2])$$

correspondingly.

To simulate the realistic shape of the myosin head and at the same time to ensure fast Fourier transform calculations, we approximated the S-1 structure found by Rayment et al. (1993) by 13 spheres. We found that for the low-angle calculations, our approximation of the S-1 shape is reasonable. To demonstrate this, we calculated six myosin layer lines from two models that have the same cross-bridge space configuration, but the heads represented at different levels of resolution. In the first model the structure of S-1 is approximated by small spheres representing individual amino acid residues located according to the crystal structure of S1 (Rayment et al., 1993). The second model is our simplified model of the cross-bridge (Fig. 2 *A*). As one can see from Fig. 2 *B*, the Fourier transforms of the models are similar in the diffraction area of interest.

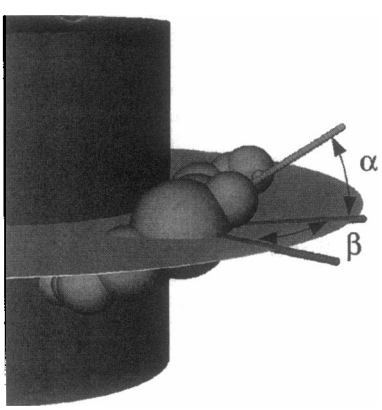

FIGURE 1 Myosin subfragment-1 (S-1) shape approximation, and space coordinates used to describe the configuration of single myosin head. S-1 is represented by 13 spheres located in such a way as to simulate the shape of a crystallographically determined structure (Rayment et al., 1993). The radial position of S-1, r_c, is determined by the distance between the center of mass (*largest sphere*) and the center of filament. α, tilt angle of the axis going through the center of mass (*largest sphere*) and actin site on the S-1 (*smallest sphere*) relative to the plane perpendicular to the filament axis; β, azimuthal angle.

RESULTS

The influence of temperature (in the range from 1°C to 30°C) on the relaxed skinned rabbit psoas muscle at ionic strength of 170 mM was studied systematically. The x-ray diffraction patterns underwent dramatic changes through a narrow range of temperature at ~14 ± 3°C (Fig. 3 *A*). Clearly defined myosin-based layer lines begin to appear at ≈12°C. The patterns can be generally categorized into two different types; one type is produced at temperatures higher than 20°C ("room temperature type"), another type at temperatures lower than 10°C ("low temperature type"). The muscle fibers remained relaxed throughout the range of temperatures used, as evidenced by the stable tension trace shown in Fig. 3 *B*. The room temperature type exhibits a strong myosin-based system of layer lines (LL1, LL2, LL3, . . .) with the 429 Å period (Fig. 3 *D*). At low temperature the myosin layer lines decrease in intensity considerably and diffuse scattering increases (Fig. 3 *C*) (see also Xu et al., 1997). There are meridional reflections on all of the layer lines, indicating that the true axial period of cross-bridge crowns is 429 Å. These results are in general agreement with the earlier reports (Wray, 1987; Wakabayashi et al., 1988; Lowy et al., 1991; see also Xu et al., 1997).

The diffraction patterns at room temperature

Data analysis

For quantitative analysis the intensity profiles along the off-meridional regions of myosin-based layer lines (Fig. 4) were taken as it was described in the Methods. There was little indication of lattice sampling except on the third layer line, one peak appears in the region close to meridian (≈0.0015 $Å^{-1}$) and another one near ≈0.004 $Å^{-1}$. The weak sixth layer line also showed some sampling. For this reason the third and the sixth layer lines were excluded from the analysis of intensity distributions and from modeling (see Discussion).

The first layer line profile has three clear maxima at the reciprocal radial positions, R, of 0.0047, 0.0096, and 0.013 $Å^{-1}$ (Fig. 4). Intensity at the first maximum is higher than the other two approximately by a factor of four. The spacing of the peak in the axial direction is very close to 429 Å, indicating that the intensity comes from the myosin component. The two other peaks are shifted slightly in the axial direction toward the actin 365 Å period. We have shown earlier (Xu et al., 1997) that the shift was most likely due to

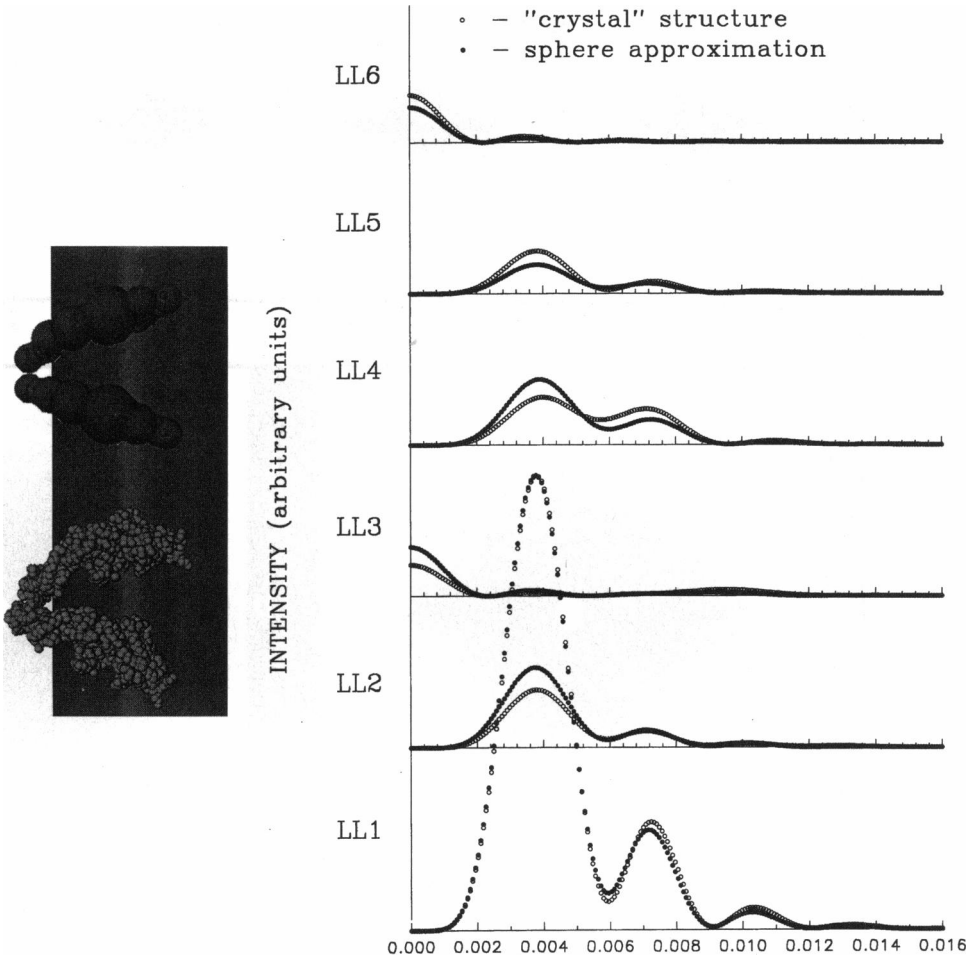

FIGURE 2 Comparison of calculated diffraction patterns using two different models of myosin subfragment-1 (S-1) structure. In the first model S1 is approximated by small spheres representing all amino acid residues that are arranged according to the crystallographic data (Rayment et al., 1993). In the second model the S1 shape is approximated by 13 larger spheres to reduce Fourier transform calculations. (*A*) Three-dimensional representation of the two models. (*B*) Calculated intensities of the first six layer lines from the two models presented in (*A*).

an intensification of the first actin-based layer line, as a result of cross-bridges weakly attached to actin.

The second and fourth layer lines have two quite well defined maxima at radii of 0.0045 $Å^{-1}$, 0.0089 $Å^{-1}$, and at radii 0.0051 $Å^{-1}$ and 0.0093 $Å^{-1}$, respectively. Only one peak can be detected on the fifth layer line at 0.0058 $Å^{-1}$ that could be at an averaged position of two unresolved maxima.

Modeling

The modeling procedure consisted of a systematic search of values of the six parameters, α_1, β_1, α_2, β_2, r_c, and Δ, based on the criteria of best fit to the intensities and spacings of the first maxima on the first, second, fourth, and fifth layer lines (LL1, LL2, LL4, and LL5). The space angles of the heads were varied with the step of 1° in the following ranges: $-90° \le \alpha_1, \alpha_2 \le -90°$, $-90° \le \beta_1, \beta_2 \le 90°$; r_c and Δ were changed with the step of 1 Å in the range of 100 Å $\le r_c \le$ 200 Å and 0 Å $\le \Delta \le$ 200 Å. The selection criteria for searching for the appropriate models were as follows. The calculated intensities were normalized by taking the first intensity peak on the LL1 as 100%. The model was considered acceptable if the intensities of the first maxima on the layer lines satisfied the following criteria: $I_{LL1} = 100$, $10 \le I_{LL2} \le 25$, $10 \le I_{LL4} \le 25$, $4 \le I_{LL5} \le 15$. For the spacings of the first maxima the criteria were: 0.0046 $Å^{-1} \le R_{LL1} \le$ 0.0048 $Å^{-1}$, 0.0042 $Å^{-1} \le R_{LL2} \le$ 0.0048 $Å^{-1}$, 0.0046 $Å^{-1} \le R_{LL4} \le$ 0.0058 $Å^{-1}$, 0.0046 $Å^{-1} \le R_{LL5} \le$ 0.0058 $Å^{-1}$.

The searching procedure described above resulted in a limited number of models that have parameters in the following range: $\alpha_1 = 25 \pm 4°$ and $\alpha_2 = -10 \pm 4°$; $\beta_1 \approx \beta_2 = 85 \pm 5°$; $r_c = 135 \pm 2$ Å, $\Delta_z = 20 \pm 2$ Å, and $\Delta_r = 16 \pm 2$ Å. Characteristic layer line profiles calculated for the average parameters are shown in Fig. 4. Good agreement with experiments can be seen on the LL1, LL2, and LL4 with the peak intensities and their radial spacings very close to those measured. The intensity of the LL5 is slightly weaker than expected and has two peaks. The *R*-factor ($\Sigma I_{obs} - I_{cal} / \Sigma I_{obs}$) calculated for the model with average parameters shown above is of the order of 6% if two intensity peaks on the LL1, LL2, LL4, and LL5 were taken into account. The calculated diffraction, however, gives the intensity of the third layer line, LL3, much weaker than the observed value. Three-dimensional representation of the model is shown in Fig. 5 *a*. The main interesting features of the model are the following. The cross-bridges are located very close to the surface of the thick filament backbone, since the backbone has an outer radius of ~90 Å (Squire,

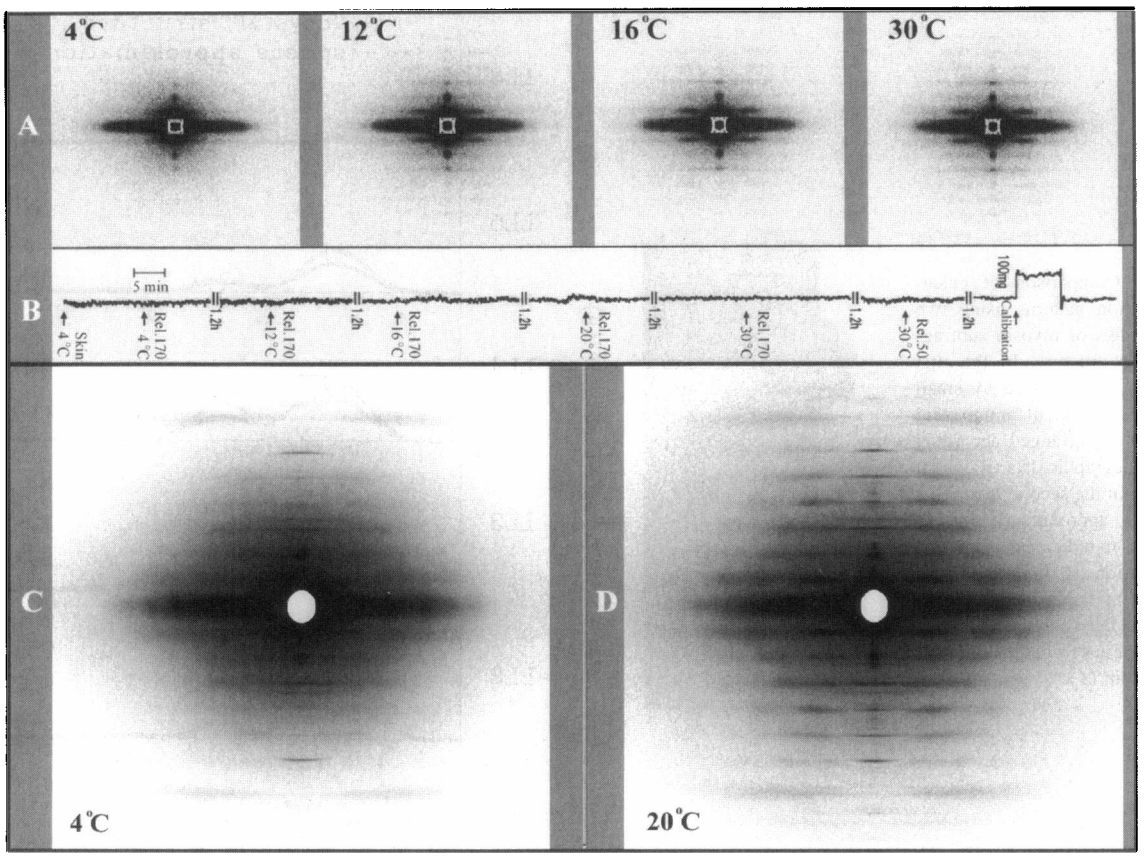

FIGURE 3 X-ray diffraction patterns recorded from single bundles of skinned, relaxed rabbit psoas muscle fibers at different temperatures. (*A*) Patterns from a bundle (0.4 mm × 0.7 mm) at μ = 170 mM with temperature ranging between 4°C and 30°C. From left to right: 4°C, 12°C, 16°C, 30°C. Reversible transition occurs within a narrow range around 14°C. Data obtained using a laboratory x-ray source and recorded on a MAR Research imaging plate detector system (Hamburg, Germany). One-hour exposure for each pattern. (*B*) Tension record from the same bundle while recording the x-ray diffraction patterns of panel *A*. Little or no tension developed with the rising temperature from 4°C to 30°C. The estimated maximal active force of the bundle would be 2 *g* (4°C) or 4 *g* (20°). *Skin*, skinning solution; *Rel.170*, relaxing solution (μ = 170 mM); *Rel.50*, relaxing solution (μ = 50 mM). (*C*) and (*D*) X-ray diffraction patterns obtained from bundles in the relaxing solution at μ = 150 mM by using synchrotron radiation on beamline X13 of EMBL at DESY, Hamburg, Germany. (*C*) At 4°C, averaged pattern from two sets of experiments. (*D*) At 20°C, averaged pattern from three sets of experiments. The patterns are displayed in logarithmic scale. The patterns can be generally categorized into two different types, one type is produced at temperatures lower than 10°C ["low T type" (*C*)], another type at temperatures higher than 20°C ["room T type" (*D*)]. At low temperature the myosin layer lines are weak and diffuse scattering is high. The room temperature type of the patterns exhibits a strong myosin-based system of layer lines with the 429-Å period.

1981) while the heads are only 135 Å (r_c) away from the center of the filament. The best fit value for the β angles of the heads is close to 90°. At these values of parameters, both heads appear to wrap around the backbone and make the filament a very compact structure as a whole.

The diffraction patterns at low temperature

Data analysis

Analysis of the low-temperature (4°C, μ = 150 mM) x-ray diffraction patterns is much more difficult. The layer lines under this condition become weak while the diffuse scattering increases considerably. The procedure used to reveal the radial profiles of the myosin layer lines obtained at room temperature cannot be applied. The second approach described in Methods was found to be more appropriate. Regularly spaced vertical cuts perpendicular to layer lines were taken, the background was subtracted from each slice, and the intensity profiles of LL1, LL2, LL4 and LL5 were reconstructed (see Fig. 6). The layer lines LL3 and LL6 are found to be too weak for analysis. The radial positions of the peaks on LL4 and LL5 are poorly defined and can hardly be measured. The second layer line has a weak indication of the lattice sampling, weaker than that at low μ, and the same temperature (Xu et al., 1997).

In Fig. 7 the intensity distribution along the first layer line is shown in contrast to the intensity of the same layer line at room temperature. The results were obtained from the same sets of muscle bundles so that one may make a direct comparison. The main differences between the two states are the following. At 4°C the amplitude of the first maximum at LL1 decreases approximately by a factor of 3.5–4, compared to that at 20°C. The radial position of the maximum is shifted toward the meridian and is located at

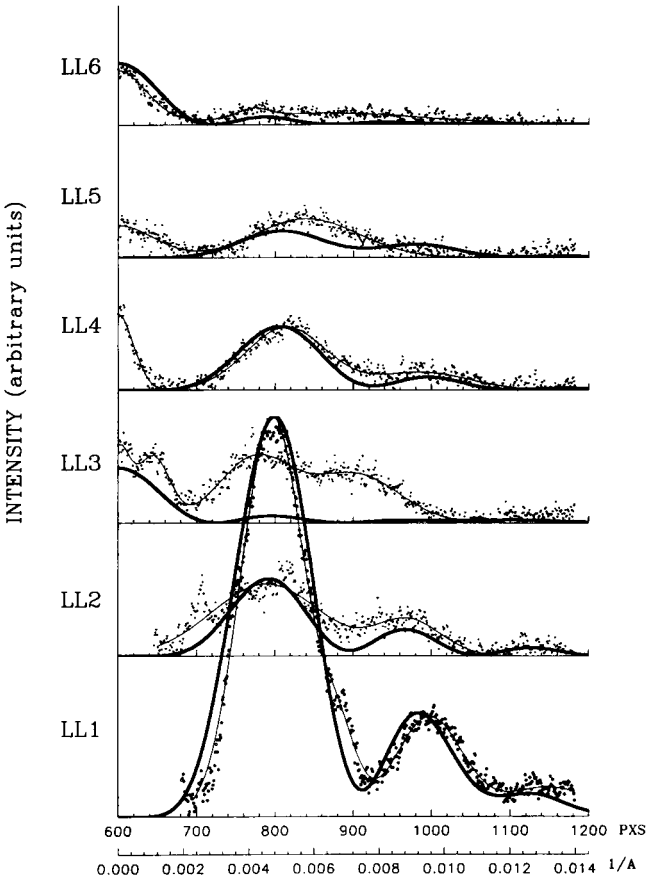

FIGURE 4 Intensity profiles along the first six myosin layer lines from the 20°C, μ = 150 mM, data set shown in 3 *D*. Scattered points represent experimentally measured (see Methods) intensity distributions along the layer lines obtained from relaxed rabbit psoas muscle at room temperature. Thin lines are obtained by a fitting procedure of the experimental points. Thick lines are calculated Fourier transforms from the best fitted model of the thick filament with the following parameters: $\alpha_1 = 25 \pm 4°$ and $\alpha_2 = -10 \pm 4°$; $\beta_1 = \beta_2 = 85 \pm 5°$; $r_c = 135 \pm 2$ Å, $\Delta_z = 20 \pm 2$ Å and $\Delta_r = 16 \pm 2$ Å. The fitting was performed for the layer lines LL1, LL2, LL4, and LL5. The LL3 and LL6 show the filament lattice sampling and probably include scattering from the backbone of the thick filaments.

0.0038–0.0039 $Å^{-1}$. The layer lines LL2, LL4, and LL5 become very weak, but their intensities relative to that of the LL1 do not appear to change significantly from those found at room temperature.

Modeling

The shift of the maximum on the first layer line indicates that the cross-bridges move radially away from the surface of the backbone. The first step in modeling was to check whether this radial movement of the cross-bridges can account for the changes in peak position and intensity on the first layer line.

A test with the same model used above shows that the radial peak shift on the first layer line from 0.0047 to 0.0038 $Å^{-1}$ can be accounted for by cross-bridge movement in the radial direction from 135 to 175 Å. However, the intensity of the peak is predicted to *increase* approximately by a factor of 1.5, contrary to the behavior found in experiments. The intensification of the first maximum occurs with all configurations of the cross-bridges we modeled, provided that the disordering factor remains unchanged.

Attempts were made to compensate for the predicted intensity increase as a result of outward movement of cross-bridges by increasing the disordering factor of the cross-bridges. To reduce the intensity of the first peak on the first layer line by a factor of 3.7 (experimental measurement) while cross-bridges move radially outward, it is necessary to increase the disordering factor, Δ, from 20 Å (for room temperature) to ~50 Å (for low temperature). While a reasonable fit for the first layer line can be found by this approach, all other higher-order layer lines completely disappear (<1% of the intensity of LL1). The actual intensities of the layer lines LL4 and LL5 are, however, ~10–15% of the intensity of the first layer line (Fig. 7). Therefore, an increase in disorder within the entire cross-bridge population does not appear to be the only cause for the decrease in the layer line intensities.

The coherent cross-bridge mass affects the absolute intensity of layer lines while the disordering factor affects the relative intensity between the first and the higher-order layer lines. One possibility is that the number of helically ordered cross-bridges that scatter coherently decreases considerably when temperature is lowered. As a next logical step, the effective mass of the ordered cross-bridge fraction was allowed to change. The result of the fitting (Fig. 5 *b* and Fig. 7) shows that at low temperature the total mass of the ordered fraction of cross-bridges should decrease by a factor of two or possibly even larger, while the disordering factor, Δ, does not increase above 25 Å, such that other layer lines show reasonable intensities.

Although the radial shift of the cross-bridges is certain, the intensities of the higher-order layer lines at low temperature are so weak that the statistics of the intensity profiles of the layer lines are very poor, rendering detailed modeling rather difficult. For example, the first maximum of the first layer line is not very sensitive to the azimuthal angles β_1 and β_2. Without sufficient data from higher-order layer lines, it is difficult to draw any definitive conclusions about changes in the orientations of the cross-bridges with temperature transitions.

DISCUSSION

By using synchrotron radiation and an imaging plate for recording diffraction patterns and by taking special precautions to prevent muscle from activation or radiation damage (see Methods), we obtained high resolution x-ray patterns from rabbit psoas muscle under relaxing conditions over a wide range of temperatures. This allowed us to obtain, for the first time, the intensity profiles of major myosin layer lines and apply a model-building approach for structural analysis.

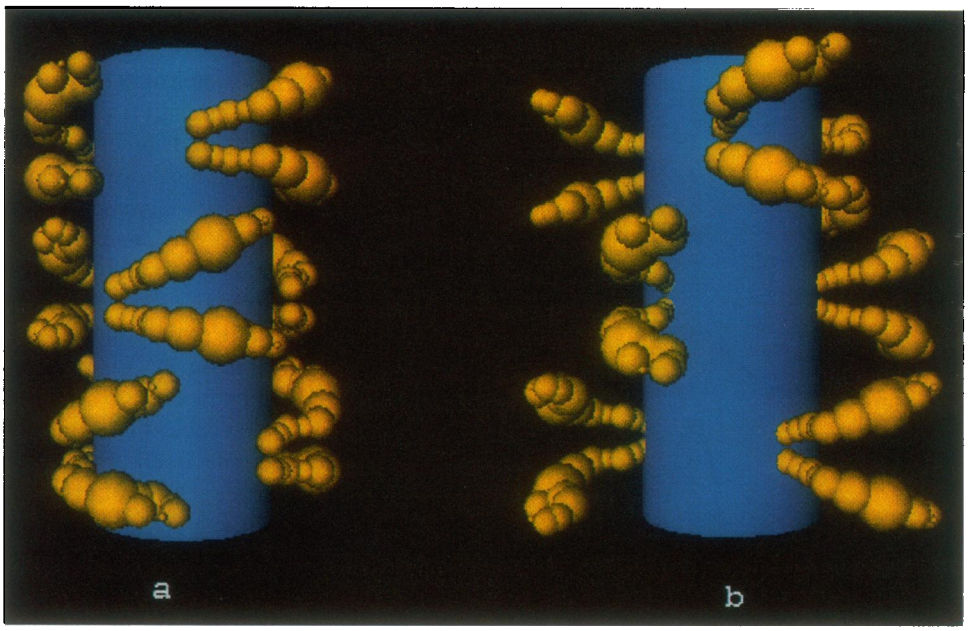

FIGURE 5 Three-dimensional representation of the thick filament at different temperatures. Modeling is based on data obtained at μ = 150 mM. (*a*) Structure of the filament at 20°C. The myosin heads are tilted in opposite directions and wrap around the filament backbone. The center of mass of the heads is located ~135 Å from the center of the filament. (*b*) Tentative structure of the filament at 4°C. The cross-bridges move radially away from the center of the filament and are located ~175 Å from the filament center. Only about half of the population helically ordered at room temperature remains ordered at low temperature. The space configuration of the myosin heads, α_1, α_2, β_1, β_2, cannot be determined due to layer lines LL2, LL4, and LL5 being very weak.

At room temperature, the x-ray pattern from rabbit psoas muscle is very similar to that from stretched frog semitendinosus muscle under relaxing conditions (Haselgrove, 1980; Malinchik and Lednev, 1987, 1992). In the case of frog muscle, the cross-bridges are located radially at 125 Å, while in the rabbit muscle they are at 135 Å, as determined by the main strong maxima on the first layer lines. In both muscles the myosin layer lines LL1, LL2, LL4, and LL5 all have the first maximum at ~1/200 Å^{-1} and the second maximum around 1/100 Å^{-1}. This feature suggests that the space configurations of the two myosin subfragments-1 (S-1) of each cross-bridge are very likely distributed in mirror symmetry relative to the plane perpendicular to the filament axis, e.g., $\alpha_1 \sim -\alpha_2$, $\beta_1 \sim \beta_2$ (Haselgrove, 1980). It means that the two myosin heads are tilted at approximately the same angle, but in opposite directions.

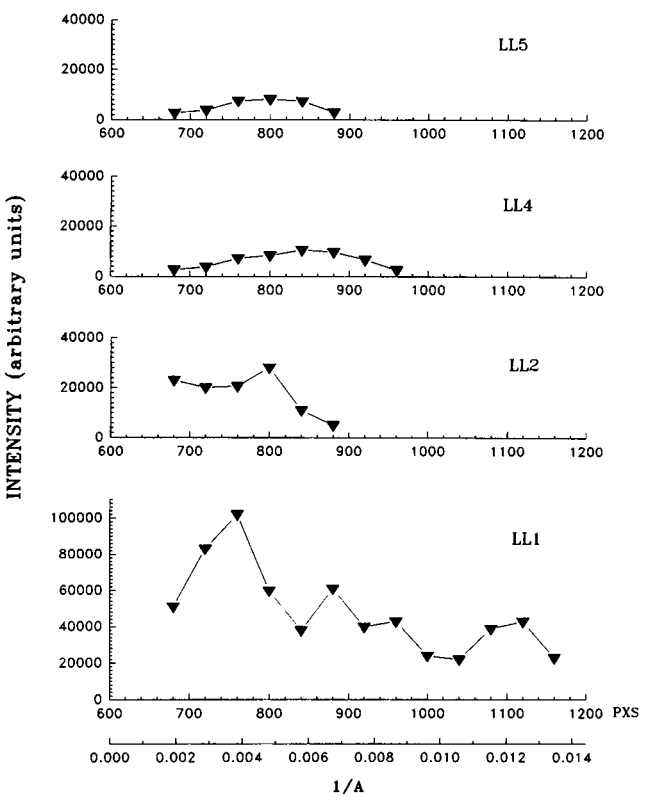

FIGURE 6 Relative intensities of myosin layer lines LL1, LL2, LL4, and LL5 at low temperature. The profiles are obtained by making regular vertical cuts (0.001 Å^{-1}) parallel to the meridian as it is described in Methods. The maxima on the profiles are defined very poorly except the one on the first layer line. The intensity on the LL4 and LL5 is ~10–15% of the main maximum on the first layer line.

In our modeling all parameters describing the space configuration, α_1, β_1, α_2, β_2, and r_c, were allowed to change independently to explore all possible values. The result of the fitting procedure gave unequal values of tilt angles, $\alpha_1 \approx 25°$ and $\alpha_2 \approx -10°$, but $\beta_1 \cong \beta_2$. The reason for $\alpha_1 \neq \alpha_2$ is evidently related to the fact that there is an experimentally measured small difference in the radial positions of maxima on LL1, LL2, LL4, and LL5 (Fig. 4).

We did not explore the additional parameters allowing each head to rotate around its long axis. The reasons are the following: 1) taking the shape of the head into account, the rotation would mainly rotate the tail of the head, which includes a relatively small part of the total mass. Our calculations showed (unpublished data) the position of the tail has little effect on intensities. The radial positions of the maxima on LL1, LL2, LL4, and LL5 are determined by the configuration of the main part of the cross-bridge. 2) Very similar values for α_1, β_1, α_2, and β_2 were obtained for the straight cylindrical shapes of the heads (unpublished data); i.e., at the present resolution, the intensity distribution is not very sensitive to the orientation of the myosin head with respect to the rotation around its long axis. The key finding

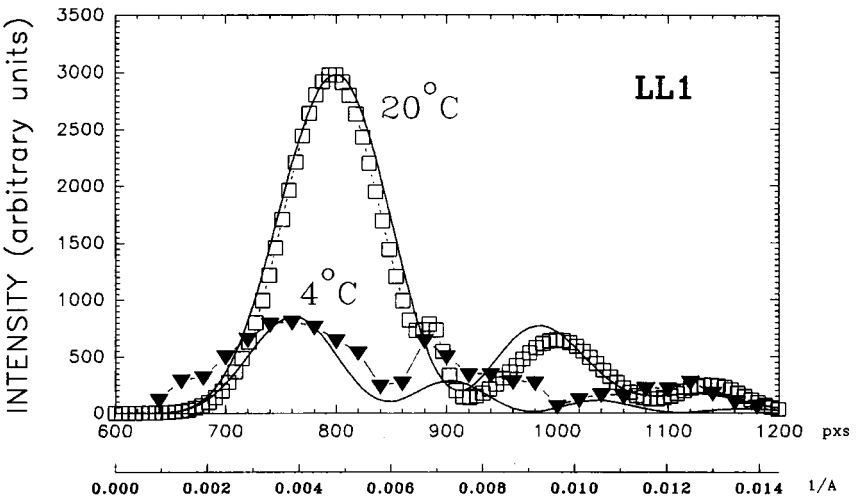

FIGURE 7 Temperature sensitivity of the first layer line intensity distribution (μ = 150 mM). For the profile at 4°C, vertical cuts were 0.0005 $Å^{-1}$ in width. The smooth curve at 20°C is the best fit curve to experimental data (same as Fig. 4). Changing temperature from room temperature to 4°C causes the first maximum on the layer line to move radially from 0.0047 to 0.0038 $Å^{-1}$ and to decrease in intensity by a factor of three to four. Our model-building studies (*smooth curve*) indicate that the changes observed can be accounted for by the cross-bridges moving radially from 135 to 175 Å while the fraction of helically ordered cross-bridges along the thick filaments decreases at least by a factor of two. (A small narrow peak in the region of 0.007 $Å^{-1}$ may originate from diffraction on the thin filaments.)

is that the myosin heads are situated close to the backbone ($\beta \approx 80°$). 3) The similarity between our simplified 13-sphere S1 model and the atomic structure of S1 in terms of diffraction effects is limited and ends at the level of rotational effects. Even if the rotational angles can be found by fitting a configuration of the 13-sphere model, the result may not correspond to the same rotational angles of the model with atomic resolution.

The present model does not show a good fit for the third layer line. There are a few possible reasons. The first possibility is that the diffraction from the backbone of single thick filament was not included in our calculation. The backbone consists of the rod regions of the myosin molecules. It has a regular axial shift of 143 Å. As a result, the electron density distribution of the backbone should be expected to be modulated in the axial direction with the 143-Å repeat. Diffraction from such structures is well known (see Vainshtein, 1966, p. 140): the layer lines with axial repeat of the 1/(143 Å) will appear. The expected intensity from the backbone of the single thick filament is quite low, but the second factor, namely sampling, due to interfilament interference, can change situations dramatically. The continuous intensities of the LL3 and LL6 are sampled by lattice Bragg reflections. The sampling is not sharp. As it usually happens, in parallel packing of long fibrils, the lattice has a liquid type of disorder, and the reflections are quite broad and may overlap. The sampling on the LL3 and LL6 can be expected even in situations when other myosin layer lines show little indication of the lattice effects. The reason is that to observe sampling on LL3 and LL6, the backbones are required only to be in a long-range axial register; for interference effects on the LL1, LL2, LL4, and LL5, the neighboring thick filaments are required, in addition, to be in azimuthal orientation order. The cross-bridges (myosin heads) are flexible and most likely do not have the required long-range azimuthal order. Therefore, the strong intensities and the sampling of LL3 and LL6 probably arise from factors other than cross-bridge distributions.

Dramatic changes take place in rabbit psoas muscle at low temperature. The x-ray diffraction pattern becomes very weak while the diffuse scattering between the layer lines increases considerably (Lowy et al., 1991; Xu et al., 1997). Our quantitative analysis is based on modeling of the first myosin layer line that remains reasonably well defined. A radial shift of the maximum toward the meridian indicates that the helically ordered population moves radially from 135 to 175 Å. However, this radial extension should be accompanied by an increase in intensity, contrary to the experimental findings. The considerable decrease in intensity cannot be explained by a simple increase in disordering of the first type for the entire population. The intensities of higher-order layer lines, for example LL4 and LL5 relative to LL1, indicate that the r.m.s. displacements of the cross-bridges scattering coherently did not change significantly. The more likely explanation is that the mass of the coherent population decreases, such that about one-half of the ordered fraction becomes disordered. It should be noted that the ordered and disordered populations coexist at all temperatures studied thus far. It is the relative ratio that is affected by temperature. Furthermore, the temperature effects on the behavior of cross-bridges do not depend on the presence of actin. Similar structural changes in the thick filament occur in the out-of-overlap region (Wray, 1987; Lowy et al., 1991; Xu, unpublished data).

The ordered and disordered cross-bridge populations differ mainly by their averaged displacements from the equilibrium positions. One fraction of cross-bridges has r.m.s. displacements of the order of 20–25 Å, scatters coherently, and produces myosin layer lines. The other one has r.m.s. displacements of the order of 100 Å or larger (our unpublished data) and produces only incoherent scattering. This conclusion is consistent with the idea of coexistence of two cross-bridge populations suggested by Poulsen and Lowy (1983) and Lowy et al. (1991) in order to interpret the myosin layer lines together with the diffuse scattering in the diffraction patterns from muscle. There is direct evidence in favor of the two cross-bridge population models from iso-

lated myosin filaments. Electron microscope studies of negatively stained myosin filaments show two configurations of cross-bridges: ordered ones located near the backbone, and disordered ones located far away from it (Knight and Trinick, 1984).

Although the original Poulsen and Lowy's concept of coexisting ordered and disordered cross-bridges is further supported by the present findings, our modeling and data analysis provide several new insights concerning the distributions of cross-bridges in the relaxed muscle: mainly, there is instead a coexistence of three populations of cross-bridges. The data show an intensification of the first actin layer line, which is most likely a result of weak attachment of the cross-bridges (Xu et al., 1997). The same study shows that in spite of significant changes in the fraction of weakly bound cross-bridges as a result of changing ionic strength, the myosin layer lines are practically unchanged, i.e., the helically ordered population is little affected. This was also observed earlier by Lowy et al. (1991). Second, the level of diffuse scattering is unaffected by the weakly bound cross-bridges, i.e., the orientation of the weak attachment is hardly distinguishable from the detached, disordered cross-bridges, and the weakly bound cross-bridges most likely form part of the disordered population. Therefore, it is concluded that cross-bridges are distributed in three populations: those that are ordered on the thick filament helix and those that are disordered; and within the disordered population, some cross-bridges are detached and some are weakly attached to actin. Since our modeling and data analysis indicate that 1) changing the temperature leads to a change in the fraction of cross-bridges located on the helix; 2) changing the ionic strength at a given temperature leads to a change in the fraction of cross-bridges weakly bound to actin [cf. Brenner (1990) and Xu et al. (1997)]; and 3) the redistributions are reversible, we further suggest that there is an equilibrium between the helically ordered, disordered/attached and disordered/detached populations of cross-bridges in a relaxed muscle fiber. The order $\leftrightarrow$ disorder distribution is primarily a function of temperature while the distribution of disordered/attached $\leftrightarrow$ disordered/detached is mainly sensitive to ionic strength at a given temperature. Furthermore, the equilibrium is dynamic, i.e., individual cross-bridges assume each of the three conformations only transiently. One observation is consistent with the idea of dynamic equilibrium: when a cross-bridge becomes disordered, it leaves a "hole" on the helix. If the holes are regularly spaced and static, the diffraction patterns would contain additional reflections other than those of helical origin (Malinchik, unpublished result), which were not observed. On the other hand, if the appearance of a hole at any site is only transient and the distribution is random at any one instant, then the time averaged diffraction patterns give rise to layer lines with reduced effective mass (Malinchik, unpublished result), which is consistent with our experimental observations.

We wish to thank Dr. Jin Gu of the National Institute of Arthritis and Musculoskeletal and Skin Diseases, National Institutes of Health, for helpful discussions.

REFERENCES

Franklin, R. E., and A. Klug. 1955. The splitting of layer-lines in X-ray fiber diagrams of helical structures. Applications to tobacco mosaic virus. *Acta Crystallogr.* 8:777–780.

Harford, J. J., and J. M. Squire. 1986. "Crystalline" myosin cross-bridge array in relaxed bony fish muscle. *Biophys. J.* 50:145–155.

Haselgrove, J. C. 1980. A model of myosin crossbridge structure consistent with the low angle X-ray diffraction pattern of vertebrate muscle. *J. Muscle Res. Cell Motil.* 1:177–191.

Holmes, K. C., D. Popp, W. Gebhard, and W. Kabsch. 1990. Atomic model of the actin filament. *Nature (Lond.).* 347:44–49.

Huxley, H. E., and W. Brown. 1967. The low-angle X-ray diagram of vertebrate striated muscle and its behavior during contraction and rigor. *J. Mol. Biol.* 30:383–434.

Ip, W., and J. Heuser. 1983. Direct visualization of the myosin crossbridge helices on relaxed rabbit psoas thick filament. *J. Mol. Biol.* 171: 105–109.

Kabsch, W., H. G. Mannherz, D. Suck, E. F. Pai, and K. C. Holmes. 1990. Atomic structure of the actin: DNAase I complex. *Nature (Lond.).* 347:37–44.

Knight, P., and J. Trinick. 1984. Structure of the myosin projections on native thick filaments from vertebrate skeletal muscle. *J. Mol. Biol.* 177:461–482.

Lowy, J., D. Popp, and A. A. Stewart. 1991. X-ray studies of order–disorder transitions in the myosin heads of skinned rabbit psoas muscles. *Biophys. J.* 60:812–824.

Malinchik, S., and V. V. Lednev. 1987. Interpretation of the X-ray diffraction pattern of skeletal muscle in resting state: 3D-model of myosin filament. *Doklady Biophysics (Proc. Acad Sci. USSR).* 293:238–242.

Malinchik, S., and V. V. Lednev. 1992. Interpretation of the X-ray diffraction pattern from relaxed skeletal muscle and modeling of the thick filament. *J. Muscle Res. Cell Motil.* 13:406–419.

Malinchik, S., S. Xu, and L. Yu. 1996. Structural transitions in relaxed skinned muscle fiber while changing temperature and ionic strength. *Biophys. J.* 70:161*a*. (Abstr.).

Poulsen, F. R., and J. Lowy. 1983. Small angle scattering from myosin heads in relaxed and rigor frog skeletal muscle. *Nature (Lond.).* 303: 146–152.

Rayment, I., W. Rypniewski, K. Schmidt-Base, R. Smith, D. R. Tomchick, M. M. Benning, D. A. Winkelmann, G. Wesenberg, and H. M. Holden. 1993. Three-dimensional structure of myosin subfragment-1: a molecular motor. *Science (Wash. DC).* 261:50–58.

Squire, J. 1981. The Structural Basis of Muscular Contraction. Plenum Press, New York.

Stewart, M., and R. W. Kensler. 1986. Arrangement of myosin heads in relaxed thick filaments from frog skeletal muscle. *J. Mol. Biol.* 192: 831–851.

Vainshtein, B. K. 1966. Diffraction of X-rays by Chain Molecules. Elsevier Publishing Co., Amsterdam.

Wakabayashi, T., T. Akiba, K. Hirose, A. Tomioka, M. Tokunaga, C. Suzuki, C. Toyoshima, K. Sutoh, K. Yamamoto, T. Matsumoto, K. Sacki, and Y. Amemiya. 1988. Temperature induced changes of thick filament and location of the functional site of myosin. *In* Molecular Mechanism of Muscle Contraction. H. Sugi and G. H. Pollack, editors. Plenum Publishing Co., New York. 39–48.

Wray, J. 1987. Structure of relaxed myosin filaments in relation to nucleotide state in vertebrate skeletal muscle. *J. Muscle Res. Cell Motil.* 8:62*a*. (Abstr.).

Xu, S., S. Malinchik, Th. Kraft, B. Brenner, and L. C. Yu. 1996. X-ray diffraction evidence that attachment conformation of weakly bound crossbridges in muscle is highly variable (nonstereospecific). *Biophys. J.* 70:290*a*. (Abstr.).

Xu, S., S. Malinchik, Th. Kraft, B. Brenner, and L. C. Yu. 1997. X-ray diffraction studies of cross-bridges weakly bound to actin in relaxed skinned fibers of rabbit psoas muscle. *Biophys. J.* 73:2655–2666.